Click-Chemistry-Mediated Synthesis of Silver Nanoparticle-Supported Polymer-Wrapped Carbon Nanotubes: Glucose Sensor and Antibacterial Material

Xuan Thang Cao,* Thao Quynh Ngan Tran, Dai-Hung Ngo, Do Chiem Tai, and Subodh Kumar

Read Online

ACCESS | Metrics & More | Article Recommendations | SI Supporting Information

ABSTRACT: We report a novel approach for the synthesis of silver nanoparticles (NPs) stabilized on polymer-wrapped carbon nanotubes (Ag@polymer/CNTs) for the non-enzymatic glucose sensing and antibacterial activity applications. Poly(styrene-*alt*-maleic anhydride) (PSM) was functionalized with amino furan to obtain furan-modified poly(styrene-*alt*-maleic anhydride) (PSMF), which was later grafted onto the surface of CNTs by Diels−Alder "click" reaction to afford a polymer/CNTs hybrid material. The photo-deposition technique was applied to immobilized small-sized (∼10 nm) AgNPs on the surface of the polymer/CNTs hybrid material using visible light irradiation. The resulting material, Ag@polymer/CNTs, showed promising electrocatalytic activity for the non-enzymatic glucose sensing and antibacterial activity in vitro assays toward *Escherichia coli*, *Staphylococcus aureus*, and *Bacillus cereus* bacteria strains. Covalent-bonded polymer layer-bearing carboxylic pendent groups to the CNTs might be playing a pivot role in not only stabilizing AgNPs but also facile electron-transfer reaction, thus demonstrating better activity.
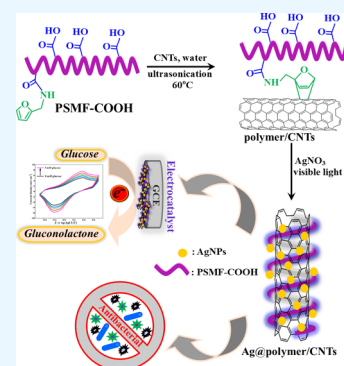
1. INTRODUCTION

Metal nanoparticles (NPs) have received a great deal of attention owing to their great applications in various fields including solar cells,[1−3] optical devices,[4,5] and catalysis.[6−8] Among them, silver nanoparticles (AgNPs) have been gaining more consideration and becoming one of the potential candidates in not only catalysis (thermal-, electro-, and photo-) but also antimicrobial therapy.[9−12] However, one of the major drawbacks for wide applicability of AgNPs is their tendency to agglomerate and thus form larger particles owing high surface energy.[13] To overcome this problem, various techniques have been proposed to control the size and stabilization of NPs during the formation process, such as inert gas condensation and cocondensation[14] and use of surfactants,[15] protecting agents,[16,17] polymeric ligands,[18,19] and biological templates.[20,21] Importantly, the activity of the resulting material depends on the size of the NPs as well as their preparation techniques.[22−24] Deposition of NPs onto a solid support is one of the important and mostly used strategies. There are various nanomaterials (organic and inorganic) that have been used as supports for the deposition of AgNPs. Carbon-based materials have been attractive owing to various unique physical and electronic properties.[25−30] Among them, carbon nanotubes (CNTs) have emerged as promising materials during the past decades due to the exceptional properties such as a huge specific surface area, electrical conductivity, and thermal stability in comparison to traditional nanomaterials.[31,32] However, the bare CNTs suffer from less functionality and thus poor dispersibility in the

reaction medium. Therefore, the surface of CNTs needs to be modified with functional groups to improve the dispersibility and provide the better stabilization for metal NPs.[33,34] In this case, the surface treatment processes by radiation and chemical oxidation using strong acids and oxidants have been mostly explored as effective strategies to improve the dispersion as well as boost binding sites.[34−37] However, these methods could disintegrate the nanotubes and generate defects in the graphitic structure, leading to a diminution in nature and properties.[38] Additionally, these methods created a large amount of highly acidic waste effluents.[39] Therefore, it is desirable to design a greener procedure for CNTs functionalization. Covalent functionalization of carbon nanomaterials including CNTs is one of the effective routes to generate the various types of organic functionalities on their surface using different types of organic moieties and polymers.[40−42] Application of organic polymers to prepare the functionalized nanomaterials is a widely used strategy. In fact, organic polymers not only stabilize and control the morphology of metal AgNPs but also integrate their own properties, which makes resulting hybrid materials a good fit for unique applications.[43−45] The deposition of AgNPs onto organic polymer-functionalized

Scheme 1. Stepwise Preparation of Ag@polymer/CNTs Hybrid Materials
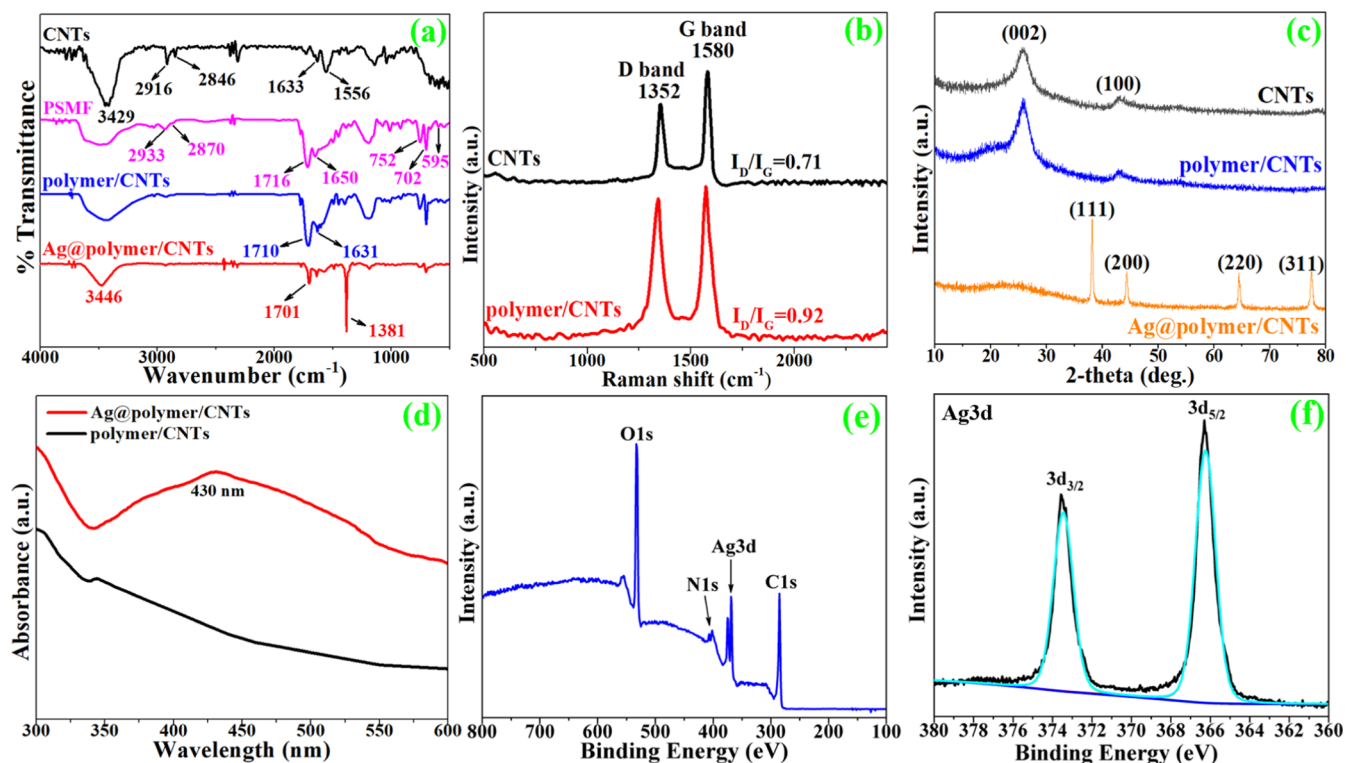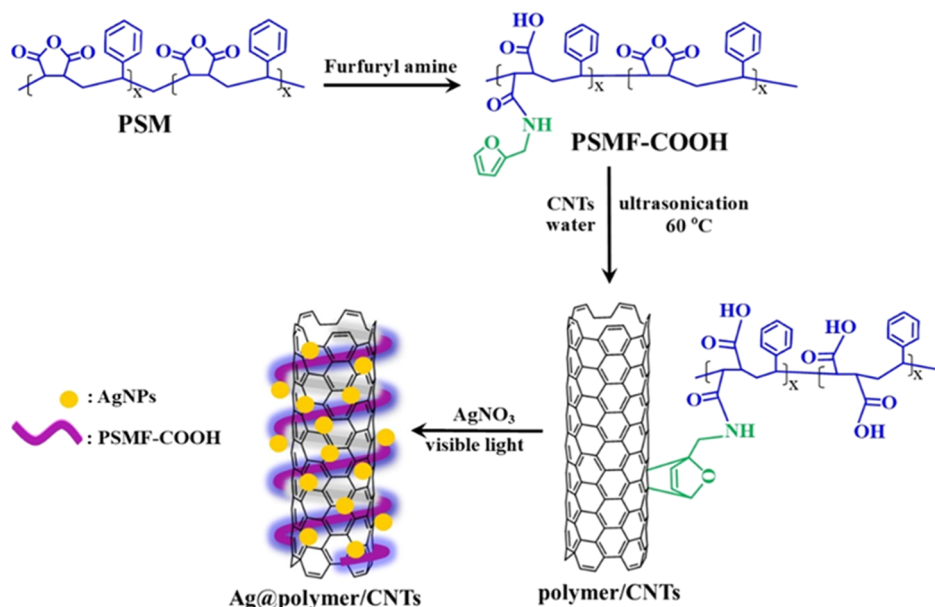
Figure 1. FTIR spectra (a), Raman spectra (b), XRD pattern (c), UV−vis spectra (d), and XPS spectra of Ag@polymer/CNTs: wide scan (e) and high resolution for Ag 3d (f).

CNTs has been widely explored for various applications such as nanocatalysts,[46] sensors,[47,48] supercapacitive electrodes,[49] and antimicrobial applications.[50] Poly(propylene imine) and polyaniline noncovalent functionalized CNTs were explored for stabilizing AgNPs.[51,52] Chitosan and pramipexole covalently bonded CNTs were used to prepare AgNPs for catalytic reduction of 4-nitrophenol and antibacterial activity.[53,54] However, these studies were carried out by using a harsh surface treatment of CNTs and reducing agents such as sodium borohydride, trisodium citrate, and dextrose. There-

fore, the covalent functionalization of CNTs using organic polymers and subsequent deposition of AgNPs under mild and environmentally friendly conditions excluding the use of harmful chemicals seems to be more appropriate in terms of sustainability.

In this work, we have synthesized AgNPs-deposited polymer-wrapped CNTs by a facile green approach involving "click" chemistry and photochemistry, which exhibited interesting electrochemical and antibacterial activities.
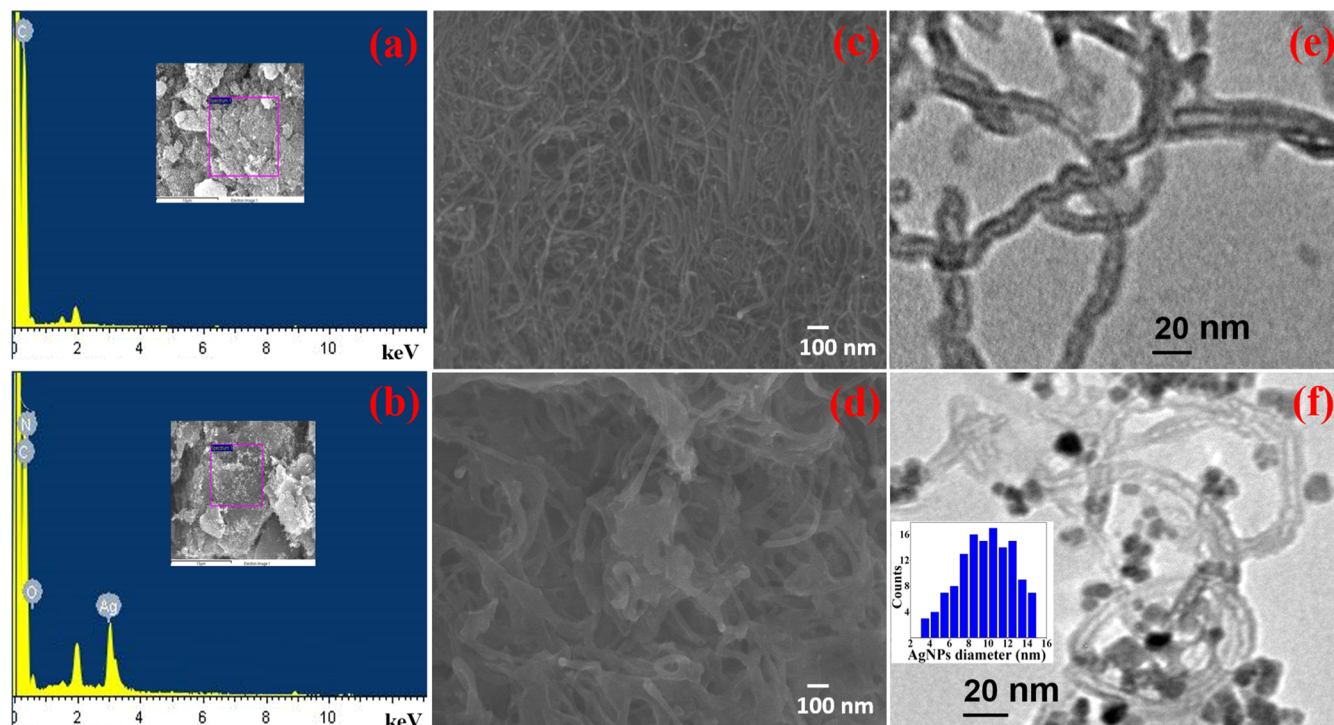
Figure 2. EDX analysis (a,b); SEM images (c,d); TEM images (e,f) of pure CNTs and Ag@polymer/CNTs with the size distribution graph (inset).

2. RESULTS AND DISCUSSION

The synthesis of the hybrid material involves three steps: (i) functionalization of poly(styrene-*alt*-maleic anhydride) (PSM) with furfural amine, (ii) grafting of PSMF-COOH (where PSMF is furan-modified PSM) to the CNTs, and (iii) photo-deposition of AgNPs. For the synthesis of Ag@polymer/CNTs, first, copolymers of PSM were functionalized with furan rings, followed by the covalent bonding to the surface of CNTs by Diels−Alder "click" chemistry in a non-catalytic aqueous solution at 60 °C under ultrasonication power. The polymer-wrapped CNTs were then used as a support material to deposit AgNPs by applying visible light irradiation without using any external reducing agents. The detailed synthesis process is shown in Scheme 1.

The synthesized material was subjected to the detailed characterization techniques such as Fourier transform infrared (FTIR) spectroscopy, X-ray diffraction (XRD), thermogravimetric analysis, scanning electron microscopy (SEM), energy-dispersive X-ray (EDX), X-ray photoelectron spectroscopy (XPS), UV−vis, transmission electron microscopy (TEM), and Raman spectroscopies. FTIR analysis showed the characteristic IR bands for the functional groups in CNTs and composites. As shown in Figure 1a, the typical peaks at 3429 and 1633 cm^{-1} for CNTs were related to O−H vibration of adsorbed moisture, while the peaks at 2916, 2846, and 1556 cm^{-1} were attributed to the C−H stretch modes and C═C bending, respectively. The absorption band at 1556 cm^{-1} was ascribed C═C vibrations of the graphitic structure. The FTIR spectrum of PSMF presented peaks for the ring-opened cyclic anhydride at 1716 and 1650 cm^{-1} and furfuryl at 595 and 752 cm^{-1}. The corresponding peaks of the polymer/CNTs composite were similarly matched with those of pristine PSMF, implying the successful functionalization onto CNTs. In the spectrum of Ag@polymer/CNTs, the intensities of

respective absorption bands remarkably decreased in comparison to those of polymer/CNTs. This result could be due to the interactions between the polymer/CNTs composite and AgNPs. In fact, a sharp peak was observed at 1381 cm^{-1} due to O−H deformations of carboxylic acid due to electrostatic attraction with AgNPs. This result suggested that carboxylic groups might be playing an important role in stabilization of AgNPs on the surface of the polymer/CNTs material. Raman analysis is one of the most powerful methods to verify the happening of Diels−Alder "click" reaction on the surface of CNTs. As shown in Figure 1b, the intensities of peaks at 1352 cm^{-1} (D band) and 1580 cm^{-1} (G band) were used to evaluate the degree of defects and crystallinity of graphitic materials. After CNTs functionalization with PSMF, the intensity ratio (I_D/I_G) increased from 0.71 to 0.92. This result could be explained by the fact that there is transition of sp^2 carbon into sp^3 carbon during the formation of covalent linkages between the furfuryl moieties of PSMF and C═C bonds on the surface of CNTs. In order to confirm the incorporation of AgNPs onto the surface of polymer/CNTs, samples were characterized by XRD (Figure 1c). The XRD pattern of the CNTs exhibited typical peaks at 2-theta values of 25.78 and 42.91°, corresponding to the (002) and (100) planes, respectively. After modifying with PSMF, the peaks of polymer/CNTs appeared at 2-theta of 25.82 and 42.71°, indicating that the graphitic structures of CNTs are still preserved. However, a broad hump near the 22° angle is the indication of polymer wrapping around the CNTs.[55] The presence of AgNPs in the Ag@polymer/CNTs composite was proved by the presence of sharp peaks at 38.16, 44.34, 64.47, and 77.41°, which are attributed to the (111), (200), (220), and (311) planes of face-centered cubic AgNPs, respectively. Moreover, the average particle size of AgNPs was calculated to be ~12.25 nm using Scherrer equation. UV−vis spectroscopy was employed as a common method to endorse the existing AgNPs. Obviously,
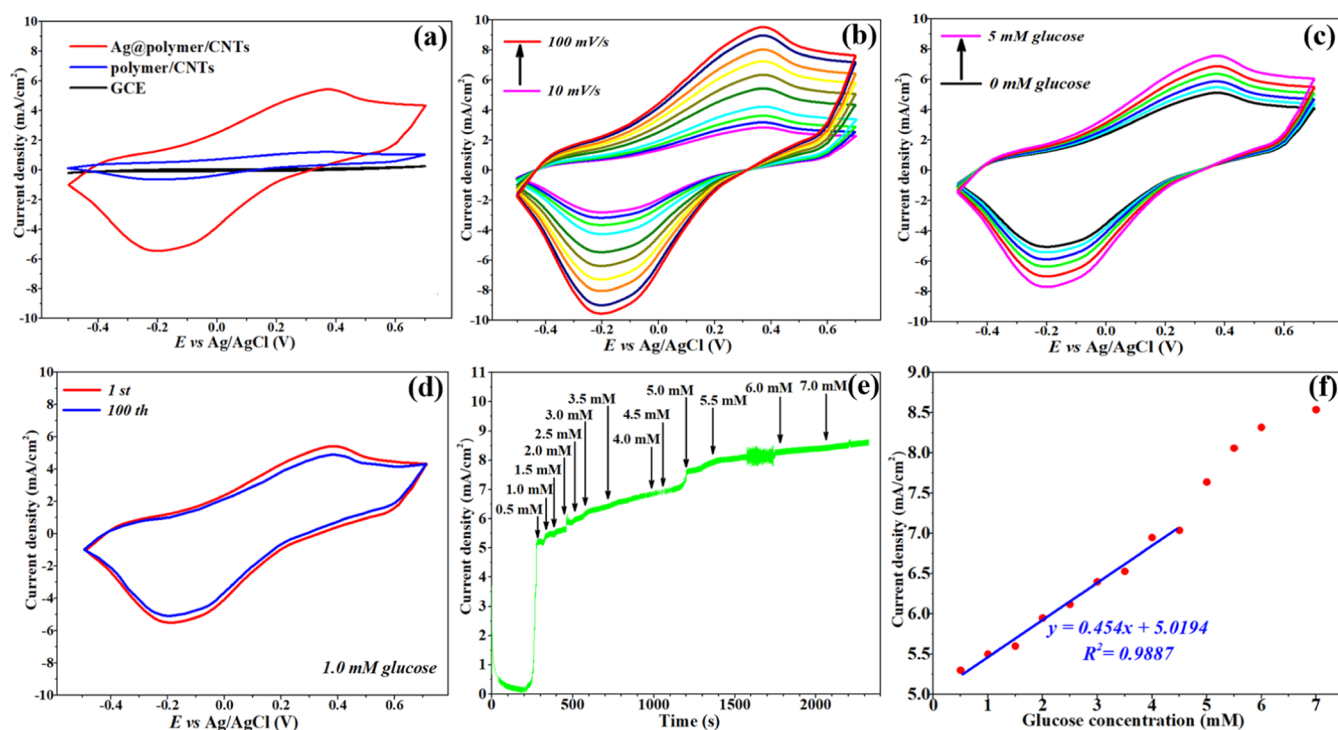
Figure 3. CV curves in 0.1 M KOH solution of bare GCE, polymer/CNTs, and Ag@polymer/CNTs in 1.0 mM glucose, scan rate 50 mV/s (a); Ag@polymer/CNTs in 1.0 mM glucose solution at different scan rates (b); Ag@polymer/CNTs in the range of 0−5.0 mM glucose, scan rate: 50 mV s^{-1} (c); Ag@polymer/CNTs after 100 cycles in 1.0 mM glucose, scan rate: 50 mV s^{-1} (d); amperometric response upon successive addition of glucose (0.5−7.0 mM) at +0.37 V applied potential (e); and linear relation of current with glucose concentration (f).

polymer/CNTs did not display any peak in the wavelength range of 400−450 nm, whereas Ag@polymer/CNTs showed a broad peak at 430 nm (Figure 1d). The appearance of this absorption peak is due to the surface plasmon resonance effect of metallic silver of a nanosize. The chemical composition of Ag@polymer/CNTs was characterized by XPS analysis. As shown in Figure 1e, wide-scan XPS spectra for Ag@polymer/CNTs presented the main peaks at binding energies of 532.96, 401.96, 368.96, and 284.96 eV, corresponding to O 1s, N 1s, Ag 3d, and C 1s, respectively. The full scan demonstrated the presence of silver element in the Ag@polymer/CNTs composite. Additionally, the high-resolution scan of the Ag 3d peak showed two peaks centered at binding energies of 366.25 and 373.48 eV, implying to Ag 3d$_{5/2}$ and Ag 3d$_{3/2}$, respectively (Figure 1f). The position of doublet peaks is attributed to the formation of metallic silver, which further indicated that silver successfully stabilized on the polymer/CNTs exists in the zero-oxidation state.

The presence of PSMF and AgNPs in the Ag@polymer/CNTs composite was analyzed by using EDX spectroscopy. As shown in Figure 2a,b, the EDX spectrum of pure CNTs showed carbon (C) as a primary element, whereas that of Ag@polymer/CNTs exhibited the peaks of carbon (C), oxygen (O), nitrogen (N), and silver (Ag), confirming the integration of PSMF polymer and AgNPs onto the CNTs. Moreover, we have used PSM polymers of different molecular weights ($M_n \sim$ 8,600, 18,900, and 29,000 g/mol). The EDX results confirmed that the use of high-molecular weight PSM polymer resulted in higher loading of AgNPs (Figure S1). These results are important in terms of controlling the loading of AgNPs, which is desirable for the catalysis/electrocatalysis applications. The morphological characteristics of the CNTs and Ag@polymer/CNTs materials are observed by SEM and TEM analysis, and

the images are shown in Figure 2. The SEM images of pristine CNTs and Ag@polymer/CNTs were clearly different due to the coated polymer layers and AgNPs on the surface (Figure 2c,d). The spherical shape of AgNPs with the size of 5−10 nm can be clearly seen in TEM images, confirming that the surfaces of polymer-wrapped nanotubes were successfully decorated with AgNPs (Figure 2f) as compared with the clean surface of CNTs (Figure 2e). In addition, the size distribution graph for AgNPs was drawn from different TEM images (Figure 2f inset). The average diameter of AgNPs was calculated to be about 9.73 nm, which is in relative agreement with the XRD data. These results confirmed the successful synthesis of Ag@polymer/CNTs.

The electrocatalytic activity of Ag@polymer/CNTs was tested for the non-enzymatic glucose sensing application. The electrochemical tests of the samples were conducted in an alkaline medium under described conditions, and cyclic voltammetry (CV) results are depicted in Figure 3. It is observed that the CV curves of bare glass carbon electrode (GCE) and polymer/CNTs did not show a redox character in the potential range from −0.5 to 0.7 V under electrochemical circumstances, whereas the Ag@polymer/CNTs presented the highest current density (mA cm^{-1}) in the presence of 1.0 mM glucose (Figure 3a). Moreover, electrochemical response toward glucose oxidation on Ag@polymer/CNTs electrode was observed at various scan rates (10−100 mV s^{-1}), as shown in Figure 3b. The intensity of the anodic peak was consistently increased with applied scan rates and shifted toward a positive voltage, implying that the first step of the glucose oxidation is a diffusion-controlled irreversible process.[56] Additionally, the current signals increased when the glucose concentration ranged from 0 to 5.0 mM (Figure 3c), indicating high sensitivity toward higher concentrations, which is obvious. The
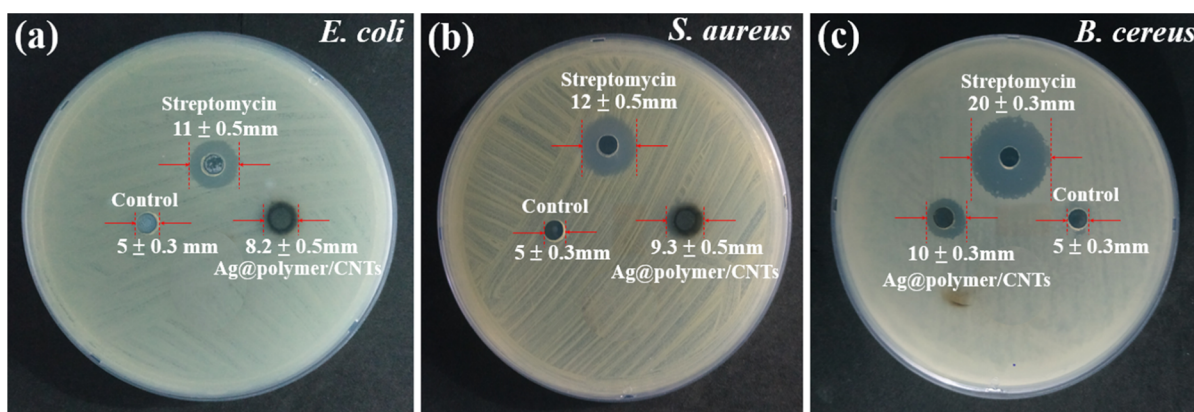
Figure 4. Inhibitory zone pattern of Ag@polymer/CNTs toward *E. coli* (a), *S. aureus* (b), and *B. cereus* (c).

current density of Ag@polymer/CNTs was found to be 5.53 mA cm^{-2} for 1.0 mM glucose, and the highest current signal was 7.64 mA cm^{-2} for 5.0 mM glucose, recorded at a scan rate of 50 mV s^{-1}. In order to compare the electrocatalytic ability of the synthesized Ag@polymer/CNTs, we have summarized several related studies in Table S1. Although experimental conditions are different from previous reports, it would give a concise idea about the performances of other metal NPs/CNTs-based electrodes. As evidenced from the table, the current density of our material is comparable with (or even better than) those of the previously reported values. The enhanced catalytic ability of the Ag@polymer/CNTs could be due its higher dispersion in the reaction medium because of the presence of many carboxyl groups on the side chain of the polymer. Moreover, smaller-sized (5−10 nm) AgNPs might also be playing an important role in improving the electrocatalytic activity by facile electron transfer. Stability of materials is one of the most important parameters for assessing the efficiency of an electrochemical process. Therefore, Ag@polymer/CNTs electrode was tested under continuous potential cycling, and the results are shown in Figure 3d. After 100 cycles, the CV curve remained in the initial shape with a slight decrease in current density, thus illustrating a stable nature of the electrocatalyst for the development of an amperometric biosensor. In order to understand the amperometric sensing behavior, chronoamperometry was performed upon successive addition of glucose from 0.5 to 7.0 mM (Figure 3e). The current signal increased continuously with higher concentrations of glucose, and the curve shifted from the left to right side during the tested time. The linear regression equation is found to be in the range of 0.5−4.5 mM, corresponding to a correlation coefficient (R^2) of 0.9887 (Figure 3f). The limit of detection and limit of quantification were calculated to be 0.375 and 1.139 mM, respectively.

Furthermore, one of the most important advantages of nanostructured silver materials is its antibacterial properties. Therefore, the antibacterial activity of Ag@polymer/CNTs was evaluated by an agar disk diffusion test. Figure 4 displays the zone of inhibition toward Gram-positive *Staphylococcus aureus* and Gram-negative *Escherichia coli* and *Bacillus cereus*. The inhibitory zones of streptomycin-resistant strains were found to be clear and wide for *E. coli*, *S. aureus*, and *B. cereus*. With treatment with Ag@polymer/CNTs, the average diameter value of the inhibitory zone was narrowed for *E. coli* (8.2 ± 0.5) mm, *S. aureus* (9.3 ± 0.5) mm, and *B. cereus* (10 ± 0.3) mm. These results illustrated that Ag@polymer/

CNTs possess effective antibacterial properties under tested concentrations toward *E. coli*, *S. aureus*, and *B. cereus*. We have also compared the antibacterial activities of our material with those of other materials reported in related papers as shown in Table S2. Although the inhibition zones toward *E. coli* and *S. aureus* are comparable with other silver/CNTs-based materials, the true comparison of the materials is not possible because of different synthesis processes, loading amounts, and material types. However, comparison can be made based on the ease of the catalyst synthesis process and its broad applicability for a quick understating to the readers. The facile synthesis process of Ag@polymer/CNTs excluding the need of any harmful reagent and its applicability toward *E. coli*, *S. aureus,* and *B. cereus* bacteria indicate that it could be a better antibacterial material.[57,58]

3. CONCLUSIONS

Ag@polymer/CNTs hybrid composites were successfully synthesized and tested for the electrocatalytic and antibacterial activities. FTIR and Raman analyses confirmed the covalent bonding of PSMF onto the surface of CNTs by Diels−Alder "click" reaction, while XRD, XPS, SEM−EDX, TEM, and UV−vis spectroscopy illustrated the incorporation of AgNPs onto the polymer/CNTs composites. The well-synthesized Ag@polymer/CNTs presented high electrocatalytic activity for the non-enzymatic glucose detection. Moreover, Ag@polymer/CNTs material exhibited effective antibacterial performances against *E. coli*, *S. aureus*, and *B. cereus*. The presence of small-sized (∼10 nm) AgNPs and carboxylic pendent groups on the side chain of the polymer might be playing a key role in enhancing catalytic activity of the material.

4. EXPERIMENTAL SECTION

4.1. Materials. CNTs (10−15 nm diameter, 10−20 μm length) were purchased from Hanwha Nanotech (Korea). PSM was synthesized according to our previous work.[59] Silver nitrate (AgNO$_3$, ≥99.8%) was purchased from Merck (Germany). Antibacterial activities of Ag@polymer/CNTs materials were investigated using three strains of bacteria, namely, Gram-positive *S. aureus*, *B. cereus,* and Gram-negative *E. coli*. The other chemicals and solvents were used as received.

4.2. Characterizations. FTIR spectra were examined using a Bruker Tensor 27 (Germany) spectrometer in the 4000−500 cm^{-1} region taking 32 scans at a resolution of 4 cm^{-1}. The samples were mixed with spectroscopic grade KBr using a mortar and compressed into pellets. XRD of materials was

recorded using a Shimadzu 6100 X-ray diffractometer (Japan) using Cu Kα radiation (λ = 1.5406 Å) at a voltage of 40 kV, a current of 30 mA, a scanning speed of 3.0°/min, and a step size of 0.02° in the 2-theta range of 10−80°. Raman spectroscopy was performed using a LabRAM spectrometer (HORIBA Jobin Yvon, Edison, NJ) with 785 nm diode laser. The morphologies of samples were observed with SEM connected with an EDX spectrometer (Hitachi JEOL-JSM-6700F system, Japan). TEM images were obtained with a JEOL JEM-2010 (JEOL, Japan) transmission electron microscope operated at 200 kV. Powder samples were dispersed in ethanol and ultra-sonicated for 5 min. One drop of this solution was placed on a copper grid with holey carbon film. The chemical states of samples were investigated using XPS (Thermo VG Multilab 2000) with monochromic Al Kα (1486.6 eV) as the X-ray source. The binding energies were calibrated with respect to the carbon 1s peak at 284.6 eV. UV−vis spectra of solutions were characterized over the wavelength range of 200−800 nm using a UV−vis spectrophotometer (METASH, China).

4.3. Preparation of PSMF. 1.0 g (4.8 mmol) of PSM and 0.24 g (2.4 mmol) of furfuryl amine were added to 7.0 mL of N,N'-dimethylformamide. The solution was purged with nitrogen for 30 min and then placed on a preheated oil bath at 60 °C for 3 h. After reaction, synthesized PSMF product was collected by precipitation in 1 M HCl (250 mL) solution and dried at 40 °C under vacuum until constant weight.

4.4. Preparation of Ag@polymer/CNTs. First, polymer/CNTs was prepared by adding CNTs (50 mg) to a homogeneous mixture of PSMF (200 mg), KOH (100 mg), and deionized water (200 mL). The resulting mixture was placed in an ultrasonication bath for 4 h at 60 °C to carry out Diels−Alder "click" reaction. The covalently bonded PSMF-wrapped CNTs was separated by centrifuge and washed with 1 M HCl (200 mL), deionized water (200 mL), and methanol (200 mL) and finally dried in vacuo at 40 °C. For the synthesis of Ag@polymer/CNTs, polymer/CNTs (20 mg) was dispersed in N,N'-dimethylformamide (15 mL), and 0.1 M AgNO$_3$ (10 mL) was then slowly added under continuous stirring. The mixture was then exposed to visible light irradiation (400−800 nm) for 2 h. The product was centrifuged and washed with deionized water and ethanol and then dried under vacuum at 40 °C.

4.5. Electrochemical Activity of Ag@polymer/CNTs for Glucose Sensing. For electrochemical measurements, the Ag@polymer/CNTs-based electrodes were investigated under ambient conditions using a potentiostat−galvanostat (VSP, BioLogic-Science Instruments, France) with and without glucose in alkaline media. A conventional three-electrode system was used with platinum wire and Ag/AgCl (3 M NaCl) corresponding to the counter and reference electrodes, respectively.

For the electrode preparation, Ag@polymer/CNTs was dispersed in ethanol (10 mg/mL) following sonication for 30 min. Then, 20 μL of the above mixture was dropped on a GCE and dried at room temperature, resulting in a uniform layer of Ag@polymer/CNTs with an active area of 7.07 mm^2. Finally, 10 μL of Nafion-117 binder solution (∼5% in a mixture of lower aliphatic alcohols and water) was dropped on the surface of Ag@polymer/CNTs-coated GCE.

4.6. Antibacterial Activity. The antibacterial activity of Ag@polymer/CNTs material was studied by the agar disk diffusion method.[60] Bacterial suspensions (10^6 cfu mL^{-1}) were swabbed evenly onto agar plates by using a sterile cotton swab.

After drying the surfaces of the plates, 50 μL of Ag@polymer/CNTs (1.5 mg mL^{-1}) along with 50 μL of streptomycin (0.1 mg mL^{-1}) as a reference in dimethyl sulfoxide was placed on the agar plates. Plates were then incubated under anaerobic conditions at 37 °C, and inhibition zone diameters were measured after 24 h.

■ ASSOCIATED CONTENT

Ⓢ Supporting Information

The Supporting Information is available free of charge at https://pubs.acs.org/doi/10.1021/acsomega.2c02832.

Comparison of the current density of the Ag@polymer/CNTs electrocatalyst and antibacterial activity with those of previously reported litrature studies (PDF)

■ AUTHOR INFORMATION

Corresponding Author

Xuan Thang Cao − *Faculty of Chemical Engineering, Industrial University of Ho Chi Minh City, Ho Chi Minh City 700000, Vietnam;* ⓞ orcid.org/0000-0002-4481-9814; Email: caoxuanthang@iuh.edu.vn

Authors

Thao Quynh Ngan Tran − *Faculty of Chemical Engineering, Industrial University of Ho Chi Minh City, Ho Chi Minh City 700000, Vietnam*

Dai-Hung Ngo − *Thu Dau Mot University, Thu Dau Mot City 820000, Vietnam*

Do Chiem Tai − *Hong Bang International University, Ho Chi Minh City 700000, Vietnam*

Subodh Kumar − *Department of Inorganic Chemistry, Faculty of Science, Palacký University Olomouc, Olomouc 77146, Czech Republic;* ⓞ orcid.org/0000-0001-8872-2785

Complete contact information is available at:
https://pubs.acs.org/10.1021/acsomega.2c02832

Notes

The authors declare no competing financial interest.

■ REFERENCES

(1) Youn, D. H.; Seol, M.; Kim, J. Y.; Jang, J. W.; Choi, Y.; Yong, K.; Lee, J. S. TiN nanoparticles on CNT-graphene hybrid support as noble-metal-free counter electrode for quantum-dot-sensitized solar cells. *ChemSuSChem* **2013**, *6*, 261−267.

(2) Zhang, J.; Lou, Y.; Zhou, H.; Zhao, Y.; Wang, Z.; Shi, L.; Yuan, S. Electrodeposited AgAu nanoalloy enhancing photoelectric conversion efficiency of dye sensitized solar cells. *Electrochim. Acta* **2019**, *324*, 134858.

(3) Maake, P. J.; Bolokang, A. S.; Arendse, C. J.; Vohra, V.; Iwuoha, E. I.; Motaung, D. E. Metal oxides and noble metals application in organic solar cells. *Sol. Energy* **2020**, *207*, 347−366.

(4) Sakhno, O.; Yezhov, P.; Hryn, V.; Rudenko, V.; Smirnova, T. Optical and Nonlinear Properties of Photonic Polymer Nanocomposites and Holographic Gratings Modified with Noble Metal Nanoparticles. *Polymers* **2020**, *12*, 480.

(5) Elemike, E. E.; Onwudiwe, D. C.; Wei, L.; Chaogang, L.; Zhiwei, Z. Noble metal -semiconductor nanocomposites for optical, energy and electronics applications. *Sol. Energy Mater. Sol. Cells* **2019**, *201*, 110106.

(6) Loza, K.; Heggen, M.; Epple, M. Synthesis, Structure, Properties, and Applications of Bimetallic Nanoparticles of Noble Metals. *Adv. Funct. Mater.* **2020**, *30*, 1909260.

(7) Rodrigues, T. S.; da Silva, A. G. M.; Camargo, P. H. C. Nanocatalysis by noble metal nanoparticles: controlled synthesis for the optimization and understanding of activities. *J. Mater. Chem. A* **2019**, *7*, 5857−5874.

(8) Davidson, M.; Ji, Y.; Leong, G. J.; Kovach, N. C.; Trewyn, B. G.; Richards, R. M. Hybrid Mesoporous Silica/Noble-Metal Nanoparticle Materials-Synthesis and Catalytic Applications. *ACS Appl. Nano Mater.* **2018**, *1*, 4386−4400.

(9) Taghavizadeh Yazdi, M. E.; Khara, J.; Sadeghnia, H. R.; Esmaeilzadeh Bahabadi, S.; Darroudi, M. Biosynthesis, characterization, and antibacterial activity of silver nanoparticles using Rheum turkestanicum shoots extract. *Res. Chem. Intermed.* **2018**, *44*, 1325.

(10) Siegel, J.; Kolářová, K.; Vosmanská, V.; Rimpelová, S.; Leitner, J.; Švorčík, V. Antibacterial properties of green-synthesized noble metal nanoparticles. *Mater. Lett.* **2013**, *113*, 59−62.

(11) Rocca, D. M.; Vanegas, J. P.; Fournier, K.; Becerra, M. C.; Scaiano, J. C.; Lanterna, A. E. Biocompatibility and photo-induced antibacterial activity of lignin-stabilized noble metal nanoparticles. *RSC Adv.* **2018**, *8*, 40454−40463.

(12) Moon, K. S.; Choi, E. J.; Bae, J. M.; Park, Y. B.; Oh, S. Visible Light-Enhanced Antibacterial and Osteogenic Functionality of Au and Pt Nanoparticles Deposited on TiO2 Nanotubes. *Materials* **2020**, *13*, 3721.

(13) Bae, E.; Park, H. J.; Lee, J.; Kim, Y.; Yoon, J.; Park, K.; Choi, K.; Yi, J. Bacterial cytotoxicity of the silver nanoparticle related to physicochemical metrics and agglomeration properties. *Environ. Toxicol. Chem.* **2010**, *29*, 2154−2160.

(14) Baker, C.; Pradhan, A.; Pakstis, L.; Pochan, D. J.; Shah, S. I. Synthesis and antibacterial properties of silver nanoparticles. *J. Nanosci. Nanotechnol.* **2005**, *5*, 244−249.

(15) AL-Thabaiti, S. A.; Al-Nowaiser, F. M.; Obaid, A. Y.; Al-Youbi, A. O.; Khan, Z. Formation and characterization of surfactant stabilized silver nanoparticles: a kinetic study. *Colloids Surf., B* **2008**, *67*, 230−237.

(16) El-Kheshen, A. A.; El-Rab, S. F. G. Effect of reducing and protecting agents on size of silver nanoparticles and their antibacterial activity. *Der Pharma Chem.* **2012**, *4*, 53−65.

(17) Kyrychenko, A.; Pasko, D. A.; Kalugin, O. N. Poly(vinyl alcohol) as a water protecting agent for silver nanoparticles: the role of polymer size and structure. *Phys. Chem. Chem. Phys.* **2017**, *19*, 8742−8756.

(18) Gur'eva, L. L.; Tkachuk, A. I.; Kuzub, L. I.; Estrina, G. A.; Knerel'man, E. I.; Khodos, I. I.; Rozenberg, B. A. Synthesis of silver nanoparticles with polystyrylcarboxylate ligands. *Polym. Sci., Ser. B* **2013**, *55*, 139.

(19) Kuzub, L. I.; Gur'eva, L. L.; Grishchuk, A. A.; Estrina, G. A.; Estrin, Y. I.; Badamshina, E. R. Regularities of the formation of silver nanoparticles with oligostyrylcarboxylate ligands. *Polym. Sci., Ser. B* **2015**, *57*, 608.

(20) Chen, P.; Wu, Q.-S.; Ding, Y.-P. Facile synthesis of monodisperse silver nanoparticles by bio-template of squama inner coat of onion. *J. Nanopart. Res.* **2008**, *10*, 207.

(21) Gopinathan, P.; Ashok, A. M.; Selvakumar, R. Bacterial flagella as biotemplate for the synthesis of silver nanoparticle impregnated bionanomaterial. *Appl. Surf. Sci.* **2013**, *276*, 717−722.

(22) Ahmad, A.; Wei, Y.; Syed, F.; Imran, M.; Khan, Z. U. H.; Tahir, K.; Khan, A. U.; Raza, M.; Khan, Q.; Yuan, Q. Size dependent catalytic activities of green synthesized gold nanoparticles and electrocatalytic oxidation of catechol on gold nanoparticles modified electrode. *RSC Adv.* **2015**, *5*, 99364−99377.

(23) Beyene, H. D.; Werkneh, A. A.; Bezabh, H. K.; Ambaye, T. G. Synthesis paradigm and applications of silver nanoparticles (AgNPs), a review. *Sustainable Mater. Technol.* **2017**, *13*, 18−23.

(24) Haider, M. S.; Shao, G. N.; Imran, S. M.; Park, S. S.; Abbas, N.; Tahir, M. S.; Hussain, M.; Bae, W.; Kim, H. T. Aminated polyethersulfone-silver nanoparticles (AgNPs-APES) composite membranes with controlled silver ion release for antibacterial and water treatment applications. *Mater. Sci. Eng., C* **2016**, *62*, 732−745.

(25) Campisi, S.; Chan-Thaw, C. E.; Wang, D.; Villa, A.; Prati, L. Metal nanoparticles on carbon based supports: The effect of the protective agent removal. *Catal. Today* **2016**, *278*, 91−96.

(26) Rivera-Cárcamo, C.; Serp, P. Single Atom Catalysts on Carbon-Based Materials. *ChemCatChem* **2018**, *10*, 5058−5091.

(27) Carabineiro, S. A. C.; Martins, L. M. D. R. S.; Avalos-Borja, M.; Buijnsters, J. G.; Pombeiro, A. J. L.; Figueiredo, J. L. Gold nanoparticles supported on carbon materials for cyclohexane oxidation with hydrogen peroxide. *Appl. Catal., A* **2013**, *467*, 279−290.

(28) Ying, C. U. I.; Yin-Jie, K.; Yin-Jie, Z.; Xiao-Hua, L. I. U.; Bo, C.; Jin-Hua, C. Spontaneous Deposition of Pt Nanoparticles on Poly(diallyldimethylammonium chloride)/Carbon Nanotube Hybrids and Their Electrocatalytic Oxidation of Methanol. *Acta Phys.-Chim. Sin.* **2013**, *29*, 989−995.

(29) Zhang, Y.; Xu, C.; Li, B.; Li, Y. In situ growth of positively-charged gold nanoparticles on single-walled carbon nanotubes as a highly active peroxidase mimetic and its application in biosensing. *Biosens. Bioelectron.* **2013**, *43*, 205−210.

(30) John, J.; Gravel, E.; Namboothiri, I. N. N.; Doris, E. Advances in carbon nanotube-noble metal catalyzed organic transformations. *Nanotechnol. Rev.* **2012**, *1*, 515−539.

(31) Rakov, E. G. The chemistry and application of carbon nanotubes. *Russ. Chem. Rev.* **2001**, *70*, 827−863.

(32) Popov, V. Carbon nanotubes: properties and application. *Mater. Sci. Eng., R* **2004**, *43*, 61−102.

(33) Jiang, H.; Zhu, L.; Moon, K.-s.; Wong, C. P. The preparation of stable metal nanoparticles on carbon nanotubes whose surfaces were modified during production. *Carbon* **2007**, *45*, 655−661.

(34) Wang, Z.; Liu, Q.; Zhu, H.; Liu, H.; Chen, Y.; Yang, M. Dispersing multi-walled carbon nanotubes with water-soluble block copolymers and their use as supports for metal nanoparticles. *Carbon* **2007**, *45*, 285−292.

(35) Lu, X.; Imae, T. Size-Controlled in situ Synthesis of Metal Nanoparticles on Dendrimer-Modified Carbon Nanotubes. *J. Phys. Chem. C* **2007**, *111*, 2416−2420.

(36) Georgakilas, V.; Gournis, D.; Tzitzios, V.; Pasquato, L.; Guldi, D. M.; Prato, M. Decorating carbon nanotubes with metal or semiconductor nanoparticles. *J. Mater. Chem.* **2007**, *17*, 2679−2694.

(37) Lu, J. Effect of surface modifications on the decoration of multi-walled carbon nanotubes with ruthenium nanoparticles. *Carbon* **2007**, *45*, 1599−1605.

(38) Shi, K.; Pang, X.; Zhitomirsky, I. Silver nanoparticle assembly on carbon nanotubes triggered by reductive surfactant coating. *Mater. Lett.* **2016**, *178*, 128−131.

(39) Dou, Y.; Liu, H.; Peng, J.; Li, M.; Li, W.; Yang, F. A green method for preparation of CNT/CS/AgNP composites and evaluation of their catalytic performance. *J. Mater. Sci.* **2016**, *51*, 5685−5694.

(40) Kumar, S.; Verma, S.; Shawat, E.; Nessim, G. D.; Jain, S. L. Amino-functionalized carbon nanofibres as an efficient metal free catalyst for the synthesis of quinazoline-2,4(1H,3H)-diones from CO2and 2-aminobenzonitriles. *RSC Adv.* **2015**, *5*, 24670−24674.

(41) Le, C. M. Q.; Cao, X. T.; Bach, L. G.; Lee, W.-K.; Kang, I.; Lim, K. T. Direct grafting imidazolium-based poly(ionic liquid) onto multiwalled carbon nanotubes via Diels-Alder ″click″ reaction. *Mol. Cryst. Liq. Cryst.* **2018**, *660*, 143−149.

(42) Le, C. M. Q.; Cao, X. T.; Tu, T. T. K.; Lee, W.-K.; Lim, K. T. Facile covalent functionalization of carbon nanotubes via Diels-Alder reaction in deep eutectic solvents. *Appl. Surf. Sci.* **2018**, *450*, 122−129.

(43) Králik, M.; Biffis, A. Catalysis by metal nanoparticles supported on functional organic polymers. *J. Mol. Catal. A: Chem.* **2001**, *177*, 113−138.

(44) Virkutyte, J.; Varma, R. S. Green synthesis of metal nanoparticles: Biodegradable polymers and enzymes in stabilization and surface functionalization. *Chem. Sci.* **2011**, *2*, 837−846.

(45) Cao, H. L.; Huang, H. B.; Chen, Z.; Karadeniz, B.; Lü, J.; Cao, R. Ultrafine Silver Nanoparticles Supported on a Conjugated Microporous Polymer as High-Performance Nanocatalysts for Nitrophenol Reduction. *ACS Appl. Mater. Interfaces* **2017**, *9*, 5231−5236.

(46) Hamedani, Y. P.; Hekmati, M. Green biosynthesis of silver nanoparticles decorated on multi-walled carbon nanotubes using the extract of Pistacia atlantica leaves as a recyclable heterogeneous nanocatalyst for degradation of organic dyes in water. *Polyhedron* **2019**, *164*, 1−6.

(47) Min, S.-H.; Lee, G.-Y.; Ahn, S.-H. Direct printing of highly sensitive, stretchable, and durable strain sensor based on silver nanoparticles/multi-walled carbon nanotubes composites. *Composites, Part B* **2019**, *161*, 395−401.

(48) Lin, J.; He, C.; Zhao, Y.; Zhang, S. One-step synthesis of silver nanoparticles/carbon nanotubes/chitosan film and its application in glucose biosensor. *Sens. Actuators, B* **2009**, *137*, 768−773.

(49) Pandit, B.; Sankapal, B. R. Highly conductive energy efficient electroless anchored silver nanoparticles on MWCNTs as a supercapacitive electrode. *New J. Chem.* **2017**, *41*, 10808−10814.

(50) Hamouda, H. I.; Abdel-Ghafar, H. M.; Mahmoud, M. H. H. Multi-walled carbon nanotubes decorated with silver nanoparticles for antimicrobial applications. *J. Environ. Chem. Eng.* **2021**, *9*, 105034.

(51) Murugan, E.; Arumugam, S.; Panneerselvam, P. New nanohybrids from poly(propylene imine) dendrimer stabilized silver nanoparticles on multiwalled carbon nanotubes for effective catalytic and antimicrobial applications. *Int. J. Polym. Mater. Polym. Biomater.* **2016**, *65*, 111−124.

(52) Deshmukh, S. P.; Dhodamani, A. G.; Patil, S. M.; Mullani, S. B.; More, K. V.; Delekar, S. D. Interfacially Interactive Ternary Silver-Supported Polyaniline/Multiwalled Carbon Nanotube Nanocomposites for Catalytic and Antibacterial Activity. *ACS Omega* **2020**, *5*, 219−227.

(53) Alshehri, S. M.; Almuqati, T.; Almuqati, N.; Al-Farraj, E.; Alhokbany, N.; Ahamad, T. Chitosan based polymer matrix with silver nanoparticles decorated multiwalled carbon nanotubes for catalytic reduction of 4-nitrophenol. *Carbohydr. Polym.* **2016**, *151*, 135−143.

(54) Hekmati, M.; Bonyasi, F.; Javaheri, H.; Hemmati, S. Green synthesis of palladium nanoparticles using Hibiscus sabdariffa L. flower extract: Heterogeneous and reusable nanocatalyst in Suzuki coupling reactions. *Appl. Organomet. Chem.* **2017**, *31*, No. e3757.

(55) Consales, M.; Cutolo, A.; Penza, M.; Aversa, P.; Giordano, M.; Cusano, A. Fiber Optic Chemical Nanosensors Based on Engineered Single-Walled Carbon Nanotubes. *J. Sens.* **2008**, *2008*, 936074.

(56) Quan, H.; Park, S.-U.; Park, J. Electrochemical oxidation of glucose on silver nanoparticle-modified composite electrodes. *Electrochim. Acta* **2010**, *55*, 2232−2237.

(57) David, M. E.; Ion, R.-M.; Grigorescu, R. M.; Iancu, L.; Holban, A. M.; Nicoara, A. I.; Alexandrescu, E.; Somoghi, R.; Ganciarov, M.; Vasilievici, G.; Gheboianu, A. I. Hybrid Materials Based on Multi-Walled Carbon Nanotubes and Nanoparticles with Antimicrobial Properties. *Nanomaterials* **2021**, *11*, 1415.

(58) Tambur, P.; Bhagawan, D.; Kumari, B.; Kasa, R. R. A facile synthesis of implantation of silver nanoparticles on oxygen-functionalized multi-walled carbon nanotubes: structural and antibacterial activity. *SN Appl. Sci.* **2020**, *2*, 981.

(59) Cao, X. T.; Vu-Quang, H.; Doan, V. D.; Nguyen, V. C. One-step approach of dual-responsive prodrug nanogels via Diels-Alder reaction for drug delivery. *Colloid Polym. Sci.* **2021**, *299*, 675−683.

(60) Mayrhofer, S.; Domig, K. J.; Mair, C.; Zitz, U.; Huys, G.; Kneifel, W. Comparison of Broth Microdilution, Etest, and Agar Disk Diffusion Methods for Antimicrobial Susceptibility Testing of Lactobacillus acidophilus Group Members. *Appl. Environ. Microbiol.* **2008**, *74*, 3745−3748.